

Magnetic Resonance Imaging of the Equine Tarsus

Marion V. Branch, BSc, PhD, Rachel C. Murray, MA, VetMB, MS, PhD,
Sue J. Dyson, MA, VetMB, PhD, and Allen E. Goodship, BVSc, PhD

Noninvasive imaging modalities for in vivo monitoring of distal tarsal osteochondral structure are needed. The objectives of this paper were to use high-field magnetic resonance (MR) imaging to describe tarsal structure, variations in association with age, exercise, and distal tarsal pain. Cadaver tarsi of specific ages and exercise histories, and from horses with a history of distal tarsal pain, were examined using MR imaging. Quantitative and subjective analysis of subchondral bone (SCB) was performed according to predefined criteria. There was a repeatable SCB thickness pattern across normal tarsi, with greatest thickness at dorsal and lateral sites. Subchondral bone thickness increased with age. High intensity exercise was associated with altered mediolateral and proximodistal thickness patterns. There was loss of the repeatable SCB thickness pattern in painful tarsi, and MR imaging detected many different types of pathology. This paper provides new information regarding structure and pathological changes in the equine tarsus, which can be used as reference material for clinical situations.

Clin Tech Equine Pract 6:96-102 © 2007 Elsevier Inc. All rights reserved.

KEYWORDS equine, tarsus, bone, joint, magnetic resonance imaging

An overview of equine tarsal anatomy using low-field magnetic resonance (MR) imaging has been published.¹ Mid-field MR imaging has been used to investigate the effect of treadmill training on the tarsal bones of Thoroughbreds.² Using high-field MR imaging lesions affecting ligaments, articular cartilage, and subchondral bone that were not evident on radiographic examination, but which may have contributed to the progression of radiographically visible distal tarsal osteoarthritis (OA), have recently been described.³

Osteochondral structure is related to the loading history of a joint, and structure varies across the joint surface.⁴ Exercise stimulates osteochondral tissue interactions, which may contribute to joint degeneration. Articular cartilage and subchondral bone (SCB) work together in their response to age and exercise. Investigation of factors that may influence or prevent disease requires validation of noninvasive imaging modalities for in vivo monitoring of distal tarsal articular cartilage and SCB.

The objectives of this paper are to: (1) describe normal anatomy of the equine tarsus using high-field MR imaging; (2) describe in detail normal distal tarsal osteochondral structure as seen using MR imaging and variations in association with age and high intensity exercise; and (3) describe structural changes in tarsi from horses with a history of distal tarsal

pain seen using MR imaging. For the purposes of this paper, the distal aspect of the tarsus is defined as the central and third tarsal bones (CT and T3) and the proximal aspect of the third metatarsal bone (MT3).

Materials and Methods

Experimental Material

The results discussed in this paper were obtained from 93 cadaver tarsi, collected from 52 horses with a variety of histories: (1) low-level exercise with no history of hind limb lameness, 5 to 17 years of age ($n = 20$); (2) Welsh section A ponies subject to pasture exercise only, 11 days of age ($n = 10$), 6 to 9 months ($n = 6$), 3 to 6 years ($n = 4$), 11 to 16 years ($n = 4$), 24 to 25 years ($n = 3$); (3) racehorses in training, 3 to 12 years of age ($n = 15$); (4) elite competition horses, 9 to 13 years of age ($n = 12$); (5) horses with distal tarsal pain and radiographic evidence of pathology, 6 to 17 years of age ($n = 16$); and (6) horses with tarsal pain and no radiographic evidence of pathology, 6 to 8 years of age ($n = 3$). Detailed history was available for every horse. Tarsal pain was localized to the distal aspect of the tarsus using local analgesia by an experienced equine orthopaedic clinician (SJD) at the Animal Health Trust, Centre for Equine Studies. The same clinician diagnosed radiographic signs of OA.

Magnetic Resonance Imaging of the Equine Tarsus

Three-dimensional gradient echo (3D GRE), spoiled gradient echo (3D SPGR) with and without fat suppression, and short

Centre for Equine Studies, Animal Health Trust, Newmarket, Suffolk (Murray, Branch, Dyson) and Royal Veterinary College and Institute of Orthopaedics and Musculoskeletal Sciences, University College, London (Goodship).

Address reprint requests to: Rachel Murray, Centre for Equine Studies, Animal Health Trust, Lanwades Park, Kentford, Newmarket, Suffolk, CB8 7UU. E-mail: rachel.murray@aht.org.uk

Table 1 Pulse Sequence Parameters Used for Imaging the Equine Tarsus

Sequence	TR (ms)	TE (ms)	Band-width	FE/PE	NEX	Slice Thickness (mm)	Interslice Spacing (mm)	FOV (cm)
Sag 3D SPGR	8.1	3.3	31.25	256/256	16.00	3	0	12
Sag 3D GRE	5.8	1.5	31.25	256/256	2.00	3	-1.5	24
Sag fast STIR	3425.0	20.0	15.63	256/192	1.00	4	1.0	22
TS 3D SPGR	8.1	3.3	31.25	256/256	2.00	3	-1.5	24
Dors 3D SPGR	8.1	3.3	31.25	256/256	2.00	3	-1.5	24

Abbreviations: Sag, sagittal; 3D, three-dimensional; SPGR, spoiled gradient echo; GRE, gradient echo; STIR, short T1 inversion recovery; TS, transverse; Dors, dorsal; TR, repetition time; TE, echo time; FE, frequency encoding; PE, phase encoding; NEX, number of excitations; FOV, field of view.

Imaging options used in all sequences were variable band width, no phase wrap, extended dynamic range, zerofill interpolation processing 512 to reconstruct the image to a 512/512 matrix, zerofill interpolation processing 2 to double the number of reconstructed slices within the prescribed range, representing a location every 1.5 mm.

T1 inversion recovery (STIR) images were acquired in sagittal, dorsal, and transverse planes using a GE Signa Echospeed 1.5 Tesla MR imaging system (General Electric Medical Systems, Milwaukee, WI). Pulse sequence parameters are summarized in Table 1.

Subchondral bone thickness was measured on high-resolution sagittal 3D SPGR images using a digital image analysis program, Scion Image (Scion Corporation, Frederick, MD). Measurements were taken at standard sites at dorsal locations 15% of the depth of T3 in the dorsal to plantar dimension on the proximal and distal aspects of both CT and T3, and the proximal aspect of MT3. Measurements were made at medial, midline, and lateral sites, which were 30%, 50%, and 70% of the width of T3, respectively. MR images were examined subjectively for the presence of abnormalities in distal tarsal osteochondral structure according to predefined criteria (Table 2).

Table 2 Criteria for the Subjective Analysis of Magnetic Resonance (MR) Images and Detection of Equine Distal Tarsal Pathology

Criteria for Analysis of MR Images

1. Irregular/poorly defined osteochondral junction
2. Focal osteochondral junction defect
3. Focal SCB abnormality
4. Irregular deep SCB border: mild
5. Irregular deep SCB border: severe
6. Abnormal ligament structure/signal intensity
7. Focal reduction in articular cartilage signal (affecting less than half the joint space in the dorsal to plantar dimension)
8. Cartilage present, but with abnormal structure/signal intensity
9. Complete loss of articular cartilage except for focal areas of high signal, and loss of joint space
10. Osteophyte formation: mild
11. Osteophyte formation: severe
12. New bone formation at capsular attachment
13. Abnormally increased area of low signal intensity dorsally: mild with trabeculae visible in cancellous bone
14. Abnormally increased area of low signal intensity dorsally: severe with no trabeculae visible in cancellous bone
15. Cystic lesion

Abbreviation: SCB, subchondral bone.

Results

Normal Tarsi

Anatomical Description of the Normal Tarsus

Normal MR anatomy of the equine tarsus is illustrated in Figs. 1-6. On 3D SPGR images, articular cartilage was a layer of homogenous intermediate signal intensity with a smooth osteochondral junction and was clearly defined from adjacent bone in all joints. Very thin cartilage and a narrow joint space prevented distinction of proximal and distal cartilage layers in the talocalcaneal-centroquartal, centrodistal (CD), and tarsometatarsal (TMT) joint spaces. However, at the mid-

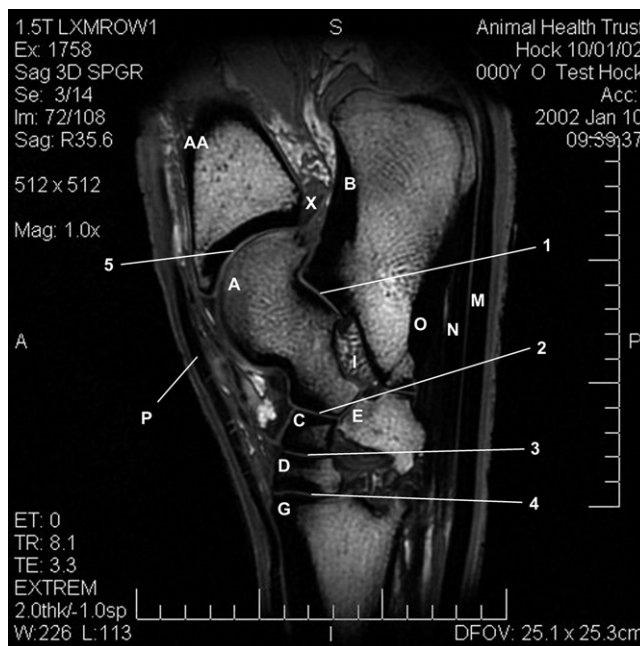


Figure 1 Lateral parasagittal 3D spoiled gradient echo image of the tarsus from a mature horse with no history of hind limb lameness, which had undergone low-level exercise. Dorsal is to the left and plantar to the right. AA, tibia; A, talus; B, calcaneus; C, central tarsal bone; D, third tarsal bone; E, fourth tarsal bone; G, third metatarsal bone; I, talocalcaneal ligament; M, superficial digital flexor tendon; N, plantar tarsometatarsal ligament; O, deep branch of plantar tarsometatarsal ligament; P, long digital extensor tendon; X, tarsocrural synovium; 1, talocalcaneal joint; 2, talocalcaneal-centroquartal joint; 3, centrodistal joint; 4, tarsometatarsal joint; 5, tarsocrural joint.

Download English Version:

<https://daneshyari.com/en/article/2393239>

Download Persian Version:

<https://daneshyari.com/article/2393239>

[Daneshyari.com](https://daneshyari.com)